IOSR Journal of Engineering (IOSRJEN) **www.iosrjen.org**
ISSN (e): 2250-3021, ISSN (p): 2278-8719
Vol. 05, Issue 08 (August. 2015), ||V4|| PP 47-59

Dufour And Heat Source Effects On Heat Mass Transfer Flow Past An Infinite Vertical Plate With Variable Thermal Conductivity

[1]I. J. Uwanta, [1]I. G. Abor and [2]Murtala Sani
[1]*Department of Mathematics, Usmanu Danfodiyo University, Sokoto-Nigeria*
[2]*Department of Mathematics and Computer Science, Umaru Musa Yar'adua University, Kasina-Nigeria*

ABSTRACT: - A numerical solution of unsteady heat mass transfer flow past an infinite vertical plate with variable thermal conductivity is presented, taking into account the effects of diffusion-thermo (Dufour number) and heat source. The influences of various parameters on the velocity, temperature and concentration profiles are studied graphically while the skin friction coefficient, Nusselt and Sherwood numbers are tabulated.

Keywords: *Heat Transfer, Mass Transfer, Thermal conductivity, Dufour Number, Heat Source, Vertical Plate.*

I. INTRODUCTION

Combined heat and mass transfer driven by buoyancy due to temperature and concentration variations is of great practical importance since there are many possible engineering applications such as; the migration of moisture through the air contained in fibrous insulation and grain storage installations and the dispersion of chemical contaminants through saturated soil. A comprehensive review on the phenomena has been recently provided by Trevisan and Bejan (1990). Double-diffusion is a type of flow driven mainly by buoyancy forces, induced by the gradients of thermal energy and concentration of a chemical component. This type of phenomena can be found in many situations in nature and engineering. In oceanography, the sea can be considered a multicomponent domain with the presence of salts and the heating of the surface starts a double-diffusive process which drives the water masses and dictates the circulation. In engineering, double-diffusion has applications in the design of solar power collectors, oil recovery and food processing, to name just a few. Therefore, it is of extreme importance the detailed understanding of the physics of this phenomena and the knowledge of which parameters affects the flow behavior.

The unsteady hydromagnetic natural convection flow on a flat translating surface with chemical reaction was considered by Al-Odat and Al-Azab (2007) who showed that both velocity and concentration are reduced by chemical reaction. Ibrahim *et al.* (2008) presented computational solutions for transient reactive magnetohydrodynamic heat transfer with heat source and wall mass flux effects. In their studies they did not consider Soret and Dufour effects which are very important characteristics in numerous chemical engineering flow domains. In view of the relative importance of these above mentioned effects, many researchers have studied and reported results for these flows which include Dursunkaya and Worek (1992), Kafoussias and Williams (1995), Anghel *et al.* (2000), Alam and Rahman (2006), Alam *et al.* (2007), Rawat and Bhargava (2009), etc. Following the study to those of Choudhary and Sharma (2006), Pantokratoras (2007) and Postelnicu (2004), Hossain and Khatun (2010) investigated the Dufour effect on combined heat and mass transfer of a steady laminar mixed free-forced convective flow of viscous incompressible electrically conducting fluid above a semi infinite vertical porous surface under the influence of an induced magnetic field. They have used the perturbation technique to solve the problem. But the numerical results were obtained only for the first order approximation.

Many physical phenomena involve free convection driven by heat generation or absorption as encountered in, for example, chemical reactor design and dissociating fluids. Heat generation effects may alter the temperature distribution and therefore, the particle deposition rate in such systems. Heat generation may also be critical in nuclear reactor cores, electronic chips, semi conductor wafers and also fire dynamics, Bég (2007). The effect of magnetic field on heat and mass transfer flows through a porous medium has also stimulated considerable interest owing to diverse applications in film vaporization in combustion chambers, transpiration, cooling of re-entry vehicles, solar wafer absorbers, manufacture of gels, magnetic materials processing, astrophysical flows and hybrid MHD power generators. Bég *et al.* (2001) used a numerical difference method to analyze the two-dimensional steady free convection magneto-viscoelastic flow in a Darcy-Brinkman porous medium.

The effects of chemical reaction on coupled heat and mass transfer flows in porous media are applicable in drying technologies, distribution of temperature and moisture over agricultural fields and groves of

fruit trees, energy transfer in wet cooling towers, flow in desert coolers and the drying and/or burnout of processing aids in the colloidal processing of advanced ceramic materials. Stangle and Aksay (1990) studied simultaneous reactive momentum, heat and mass transfer phenomena in disordered porous media with applications in optimization of processing conditions in the design of an improved binder removal process. Souza *et al.* (2003) studied mass transfer in a packed-bed reactors including dispersion in the main fluid phase, internal diffusion of the reactant in the pores of the catalyst and surface reaction inside the catalyst.
Recently, Muthucumaraswamy *et al.* (2009) studied mass transfer with a chemical reaction on unsteady flow past an accelerated isothermal vertical plate while Rajesh *et al.* (2009) studied chemical reaction and radiation effects on MHD flow past an infinite vertical plate with variable temperature.

The aim of the present study is to investigate the diffusion-thermo (Dufour number) and heat source effects on heat mass transfer flow past an infinite vertical plate with variable thermal conductivity. The dimensionless governing equations which are coupled and nonlinear were solved numerically using the implicit finite difference scheme. The effect of the parameters on the velocity, temperature and the concentration distributions of the flow fields are discussed and shown graphically while the skin friction, rate of heat and mass transfer are discussed and shown using tables.

II. PROBLEM FORMULATION

Consider a flow along an infinite vertical plate that is embedded in a porous medium. Let u' and v' be the velocity component along the x' - and y' -directions respectively. If x' - axis is chosen along the plate in the vertically upward direction and y' - axis perpendicular to it, then the investigated flow does not depends on x'. Hence, the continuity equation becomes:

$$\frac{\partial v'}{\partial y'} = 0 \tag{1}$$

Initially, the plate and the fluid are at same temperature T'_∞ with concentration level C'_∞. At time t′ > 0, the plate temperature and the mass concentration is raised to T'_w and C'_w causing the presence of temperature and concentration difference $T'_w - T'_\infty$ and $C'_w - C'_\infty$ respectively. It is assumed that both the thermal conductivity and the nth order chemical reaction are not constant and the MHD term is derived from an order-of-magnitude analysis of the full Navier-Stokes equations while the porous medium is regarded as an assembly of small identical spherical particles fixed in space. Under these conditions and assuming variation of density in the body force term (Boussinesq's approximation), the problem can be governed by the following set of equations:

$$\frac{\partial u'}{\partial t'} + v'\frac{\partial u'}{\partial y'} = \upsilon\frac{\partial^2 u'}{\partial y'^2} - \frac{\sigma B_0^2 u'}{\rho} - \frac{\upsilon u'}{k^*} + g\beta\left(T' - T'_\infty\right) + g\beta^*\left(C' - C'_\infty\right) \tag{2}$$

$$\frac{\partial C'}{\partial t'} + v'\frac{\partial C'}{\partial y'} = D\frac{\partial^2 C'}{\partial y'^2} - R^*\left(C' - C'_\infty\right)^n \tag{3}$$

$$\frac{\partial T'}{\partial t'} + v'\frac{\partial T'}{\partial y'} = \frac{1}{\rho C_p}\frac{\partial}{\partial y'}\left(K\left(T'\right)\frac{\partial T'}{\partial y'}\right) - \frac{1}{\rho C_p}\frac{\partial q_r}{\partial y'} + \frac{\upsilon}{C_p}\left(\frac{\partial u'}{\partial y'}\right)^2 + \frac{Q\left(T' - T'_\infty\right)}{\rho C_p} + \frac{D_m k_T}{C_s C_p}\frac{\partial^2 C'}{\partial y'^2} \tag{4}$$

The relevant initial and boundary conditions are:

$$\left.\begin{array}{llll} t' \le 0, & u' = 0, \quad T' = T'_\infty, & C' = C'_\infty & \text{for all } y' \\ t' > 0, & u' = 0, \quad T' = T'_\infty + \left(T'_w - T'_\infty\right)\dfrac{U_0^2 t'}{\upsilon}, & C' = C'_\infty + \left(C'_w - C'_\infty\right)\dfrac{U_0^2 t'}{\upsilon} & \text{at } y' = 0 \\ & u' \to 0, \quad T' \to T'_\infty, & C' \to C'_\infty & \text{as } y' \to \infty \end{array}\right\} \tag{5}$$

where υ is the kinematic viscosity of the grey fluid, σ is the Stefan-Boltzmann constant, B_0 is the constant magnetic field intensity, ρ is density, k^* is the permeability, g is the gravitational constant, β is the thermal expansion coefficient, β^* is the concentration expansion coefficient, T' is the temperature, C' is the mass concentration, D is the chemical molecular diffusivity, R^* is the chemical reaction, C_p is the specific heat at constant pressure, q_r is the radiative heat flux, u' and v' are velocity components in *x* and *y* directions

respectively, t' is time, K(T') is the thermal conductivity, Q is the volumetric rate of heat generation and n is the reaction order while T_w' is the wall temperature, T_∞' is the free stream temperature, C_w' is the species concentration at the plate surface, C_∞' is the free stream concentration, k_T is the thermal diffusion ratio, C_s is the concentration susceptibility and D_m is the mass diffusivity.

From the continuity equation (1), it is clear that the suction velocity is either a constant or a function of time. Hence, on integrating equation (1), the suction velocity normal to the plate is assumed in the form, $v' = -v_0$ where v_0 is a scale of suction velocity which is non-zero positive constant. The negative sign indicates that the suction is towards the plate and $v_0 > 0$ corresponds to steady suction velocity normal at the surface.

Assuming the radiative heat flux from the Rosseland approximation to have the form

$$\frac{\partial q_r}{\partial y'} = -4\sigma a^* \left(T_\infty'^4 - T'^4\right) \quad (6)$$

σ is the Stefan-Boltzmann constant, a^* is the mean absorption effect for thermal radiation constant. We assume that the temperature differences within the flow are sufficiently small such that T'^4 can be expanded in a Taylor series about T_∞' and neglecting higher order terms give

$$T'^4 \cong 4T'T_\infty'^3 - 3T_\infty'^4 \quad (7)$$

The thermal conductivity depends on temperature. It is used by Molla *et al.* (2005), as follows:

$$K\left(T'\right) = k_0\left\{1+\gamma\left(T'-T_\infty'\right)\right\} \quad (8)$$

where k_0 is the thermal conductivity of the ambient fluid and γ is a constant.

III. METHOD OF SOLUTION

To solve the governing equations in dimensionless form, we introduce the following non-dimensional quantities:

$$U = \frac{u'}{U_0}, y = \frac{y'U_0}{\upsilon}, t = \frac{t'U_0^2}{\upsilon}, \theta = \frac{T'-T_\infty'}{T_w'-T_\infty'}, C = \frac{C'-C_\infty'}{C_w'-C_\infty'}, \tau = \gamma\left(T_w'-T_\infty'\right), Du = \frac{\mathrm{D}_m k_T\left(C_w'-C_\infty'\right)}{C_s C_p \upsilon\left(T_w'-T_\infty'\right)},$$

$$Sc = \frac{\upsilon}{D}, \mathrm{Pr} = \frac{\upsilon\rho c_p}{k_0}, Ec = \frac{U_0^2}{c_p\left(T_w'-T_\infty'\right)}, Gr = \frac{g\beta\upsilon\left(T_w'-T_\infty'\right)}{U_0^3}, Gc = \frac{g\beta^*\upsilon\left(C_w'-C_\infty'\right)}{U_0{}^3}, \alpha = \frac{v_0}{U_0},$$

$$K = \frac{k^*U_0{}^2}{\upsilon}, N = \frac{16a\sigma^*T_\infty'^3\upsilon}{k_0U_0}, M = \frac{\upsilon\sigma B_0^2}{\rho U_0{}^2}, Kr = \frac{\upsilon R^*\left(C_w'-C_\infty'\right)^{n-1}}{U_0^2}, S = \frac{Q\upsilon^2}{k_0U_0^2} \quad (9)$$

The governing equations on using (9) into (1), (2), (3), (5) and using (6) - (9) into (4) reduce to the following

$$\frac{\partial U}{\partial t} - \alpha\frac{\partial U}{\partial y} = \frac{\partial^2 U}{\partial y^2} - \left(M+\frac{1}{K}\right)U + Gr\theta + GcC \quad (10)$$

$$\frac{\partial C}{\partial t} - \alpha\frac{\partial C}{\partial y} = \frac{1}{Sc}\frac{\partial^2 C}{\partial y^2} - KrC^n \quad (11)$$

$$\frac{\partial\theta}{\partial t} - \alpha\frac{\partial\theta}{\partial y} = \frac{\left(1+\tau\theta\right)}{\mathrm{Pr}}\frac{\partial^2\theta}{\partial y^2} + \frac{\tau}{\mathrm{Pr}}\left(\frac{\partial\theta}{\partial y}\right)^2 + \frac{\left(S-N\right)}{\mathrm{Pr}}\theta + Ec\left(\frac{\partial U}{\partial y}\right)^2 + \mathrm{Du}\frac{\partial^2 C}{\partial y^2} \quad (12)$$

subject to the boundary conditions

$$\begin{array}{llll} t \le 0, & U = 0, & \theta = 0, & C = 0 \quad \textit{for all } y \\ t > 0, & U = 0, & \theta = t, & C = t \quad \textit{at } y = 0 \\ & U \to 0, & \theta \to 0, & C \to 0 \quad \textit{as } y \to \infty \end{array} \quad (13)$$

where Pr is the Prandtl number, Sc is Schmidt number, Ec is Eckert number, Gr is thermal Grashof number, Gc is mass Grashof number, Du is the Dufour number, M is magnetic field, K is porosity, N is the radiation, α is suction, τ is the thermal conductivity, Kr is the chemical reaction, n is the reaction order and S is heat source parameters.

IV. NUMERICAL PROCEDURE

Equations (10) - (12) are unsteady coupled non-linear partial differential equations and are to be solved under the initial and boundary condition of equation (13). However, exact or approximate solutions are not possible for these set of equations and hence were solved by the implicit finite difference scheme. Equations (10) - (12) gives

$$-r_1U_{i-1}^{j+1}+\left(1+2r_1\right)U_i^{j+1}-r_1U_{i+1}^{j+1}=r_2U_{i-1}^{j}+\left(1-2r_2-\gamma r_3-r_4\right)U_i^{j}+\left(r_2+\gamma r_3\right)U_{i+1}^{j}+\Delta tGr\theta_i^{j}+\Delta tGcC_i^{j} \quad (14)$$

$$-r_1C_{i-1}^{j+1}+\left(Sc+2r_1\right)C_i^{j+1}-r_1C_{i+1}^{j+1}=r_2C_{i-1}^{j}+\left(Sc-2r_2-\gamma r_3Sc\right)C_i^{j}+\left(r_2+\gamma r_3Sc\right)C_{i+1}^{j}-KrSc\Delta t\left(C_i^{j}\right)^n \quad (15)$$

$$-qr_1\theta_{i-1}^{j+1}+\left(\Pr+2qr_1\right)\theta_i^{j+1}-qr_1\theta_{i+1}^{j+1}=qr_2\theta_{i-1}^{j}+\left(\Pr-2qr_2-\gamma r_3\Pr(S-N)\Delta t\right)\theta_i^{j}+\left(qr_2+\gamma r_3\Pr\right)\theta_{i+1}^{j}+\tau r_5\left(\theta_{i+1}^{j}-\theta_{i-1}^{j}\right)^2+\Pr Ecr_5\left(U_{i+1}^{j}-U_{i-1}^{j}\right)^2+\mathrm{Dur}_6\left(C_{i-1}^{j}-2C_i^{j}+C_{i+1}^{j}\right) \quad (16)$$

where $r_1=\dfrac{\alpha\Delta t}{\left(\Delta y\right)^2}, r_2=\dfrac{\left(1-\alpha\right)\Delta t}{\left(\Delta y\right)^2}, r_3=\dfrac{\Delta t}{\Delta y}, r_4=\Delta t\left(M+\dfrac{1}{K}\right), r_5=\dfrac{\Delta t}{4\left(\Delta y\right)^2}, r_6=\dfrac{\Delta t}{\left(\Delta y\right)^2}, q=1+\tau\theta_1^{j}$.

The mesh sizes along y- direction and time t-direction are Δy and Δt respectively while the index i refers to space y and j refers to time t. The finite difference equations (14) - (16) at every internal nodal point on a particular n-level constitute a tridiagonal system of equations which are solved by using the Thomas Algorithm. In each time step, the concentration and temperature profiles have been computed first from equations (15) and (16) and then the computed values are used to obtain the velocity profile which meets the convergence criteria. The skin friction coefficient, rate of heat and mass transfer in terms of Nusselt number and Sherwood number respectively are given by

$$C_f=\left(\frac{\partial U}{\partial y}\right)_{y=0},\ \mathrm{Nu}=\left(\frac{\partial \theta}{\partial y}\right)_{y=0},\ \mathrm{Sh}=\left(\frac{\partial C}{\partial y}\right)_{y=0}$$

V. RESULTS AND DISCUSSION

The numerical solutions are simulated for different values of the Prandtl number (Pr), Schmidt number (Sc), Eckert number (Ec), thermal Grashof number (Gr), mass Grashof number (Gc), Dufour number (Du), radiation (N), magnetic field (M), porosity (K), thermal conductivity (τ), suction (α), reaction order (n), chemical reaction (Kr) and heat source (S), parameters. The following parameters values are fixed throughout the calculations except where otherwise stated, Pr = 0.71, Sc = 0.62, Ec = 0.01, M = 1, K = 1, Gr = 1, Gc = 1, N = 0.1, S = 1, α = 1, τ = 0.1, Kr = 0.1, n = 1, Du = 1.

Figures 4.3.1 to 4.3.11illustrates the velocity profiles for different values of Prandtl number (Pr = 0.71, 1.63, 2.18, 7), Schmidt number (Sc = 0.22, 0.62, 1, 2.63), thermal Grashof number (Gr = 1, 2, 3, 4), mass Grashof number (Gc = 1, 2, 3, 4), magnetic field (M = 1, 5, 10, 15), porosity (K = 0.1, 0.3, 0.5, 0.7), radiation (N = 1, 5, 10, 15), suction (α = 1, 3, 5, 7), Dufour number (Du = 0.1, 1, 2, 3), chemical reaction (Kr = 0.1, 1, 10, 100) and heat source (S = 1, 3, 5, 7) parameters.

Figure 4.3.1 shows that the velocity decrease with increasing Prandtl number and Figure 4.3.2 also reveals that, the velocity decrease with increase in the Schmidt number. Likewise, Figure 4.3.3 indicates that, the velocity decreases with increase in the magnetic field parameter. But, Figure 4.3.4 pointed that, the velocity increase whenever porosity parameter increases and Figure 4.3.5 which represents the thermal Grashof number shows that, the velocity increase with increasing thermal Grashof number just like Figure 4.3.6 which reveals that, the velocity increase when the mass Grashof number increased. While from Figure 4.3.7, it shows that, the velocity

decrease with increasing radiation parameter and similarly for the suction parameter, Figure 4.3.8 indicates that, the velocity decrease with increase in the suction parameter. In Figure 4.3.9, it is seen that, the velocity increase with increasing Dufour number whereas in Figure 4.3.10 we found that, the velocity decrease when the chemical reaction parameter increase unlike Figure 4.3.11 where the velocity increases with increasing heat source parameter.

Figures 4.3.12 to 4.3.14 represents the concentration profiles for different values of Schmidt number (Sc = 0.62, 0.78, 1, 2.63), suction (α = 1, 3, 5, 7) and chemical reaction (Kr = 0.1, 1, 10, 30) parameter as in Figures 4.3.12, 4.3.13, and 4.3.14 respectively.

In Figure 4.3.12, it is observed that, the concentration decrease with increase in the Schmidt number and likewise Figure 4.3.13 shows that, the concentration decrease with increase in the suction parameter. Similarly, Figure 4.3.14 reveals that, the concentration decrease whenever the chemical reaction parameter increased.

The temperature profiles have been studied and illustrated in Figures 4.3.15 to 4.3.20 for different values of Prandtl number (Pr = 1.63, 2.18, 3, 7), radiation (N = 1, 5, 10, 15), suction (α = 1, 3, 5, 7), thermal conductivity (τ = 0.1, 1, 5, 10), heat source (S = 1, 3, 5, 7) and Dufour number (Du = 0.1, 1, 2, 3), parameters shown in Figures 4.3.15, 4.3.16, 4.3.17, 4.3.18, 4.3.19 and 4.3.20 respectively.

Figure 4.3.15 shows that, the temperature decrease with increase in the Prandtl number. Also, Figure 4.3.16 indicates that the temperature decrease with increase of the radiation parameter and similasrly for the suction parameter, Figure 4.3.17 reveals that, the temperature decrease whenever the suction parameter increased. Figure 4.3.18 shows that, the temperature increase with increase of the thermal conductivity parameters just like Figure 4.3.19, the temperature increase with respect to increase in the heat source parameter and similarly Figure 4.3.20, the temperature increase whenever the Dofour number increases.

Tables 4.3.1 to 4.3.3 are for the Skin friction coefficient, Nusselt number and Sherwood number for the numerical solution.

Table 4.3.1 illustrate the Skin friction for different values of Prandtl number Pr, thermal Grashof number Gr, mass Grashof number Gc, Schmidt number, chemical reaction Kr, suction α, magnetic field M, radiation N and S heat source parameters. From the Table, it is noticed that increase in the Prandtl number, Schmidt number, chemical reaction, suction, magnetic field and radiation parameters decrease the Skin friction but increases whenever the thermal Grashof number, mass Grashof number and heat source parameter increased.

Table 4.3.2 present the Nusselt number for different values of Prandtl number Pr, thermal conductivity τ, radiation N, suction α and n reaction order parameters. In the Table, it is observed that the Nusselt number decreases whenever any of the parameters is increased.

Similarly, the Sherwood number is demonstrated in Table 4.3.3 for different values of Schmidt number Sc, chemical reaction Kr and α suction parameters. Results from the Table shows that the Sherwood number decreases with increase of any of the parameters.

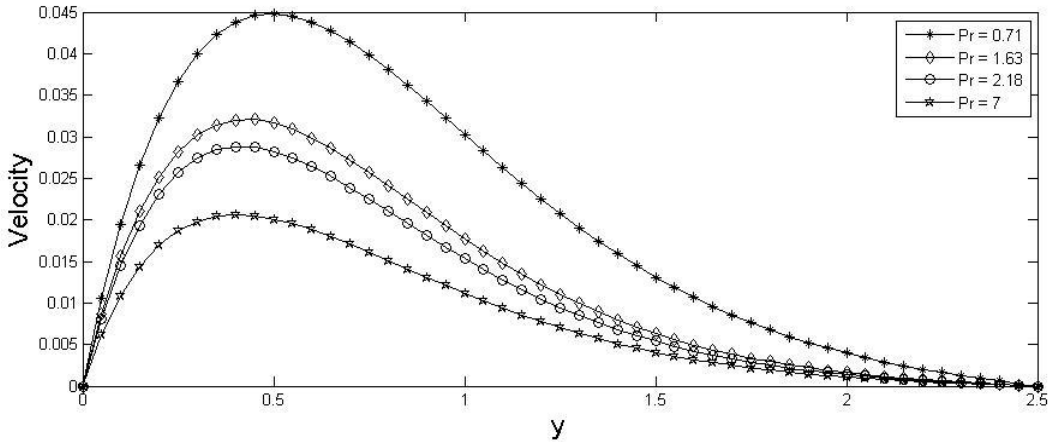

Figure 1: Variation of Velocity against y for different values of Pr.

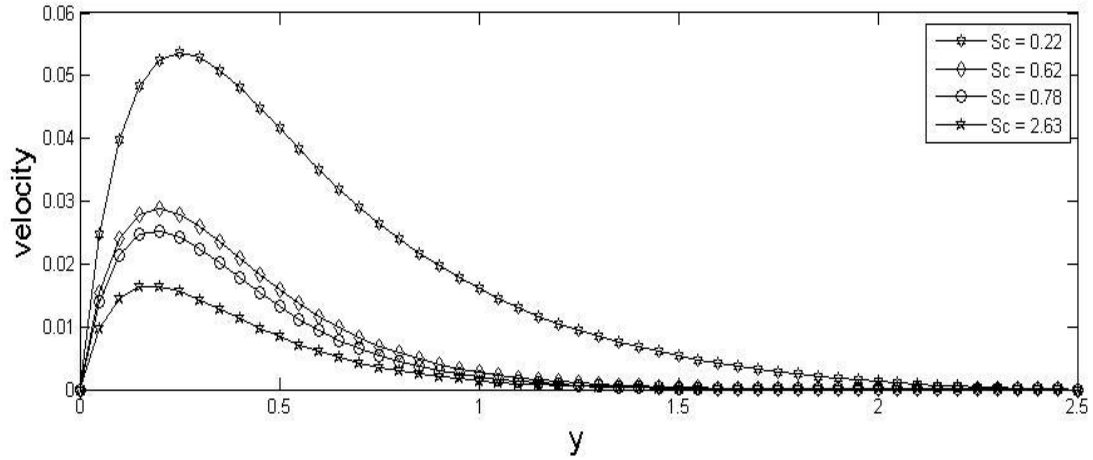

Figure 2: Variation of Velocity against y for different values of Sc.

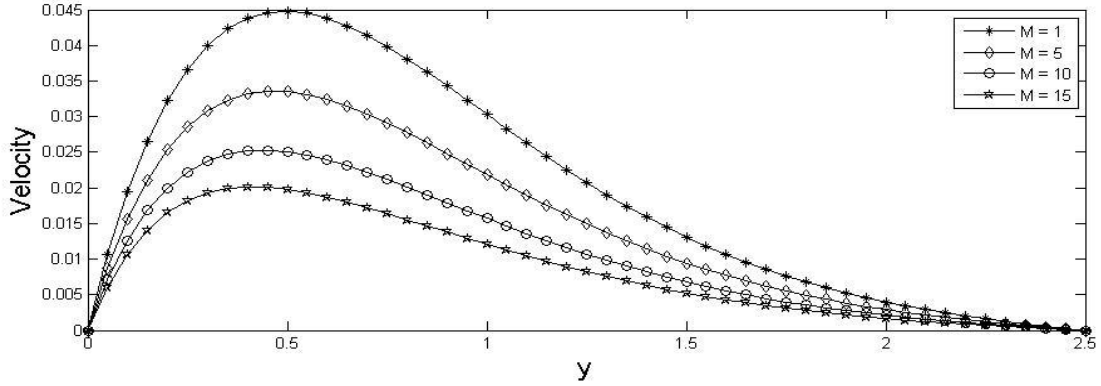

Figure 3: Variation of Velocity against y for different values of M.

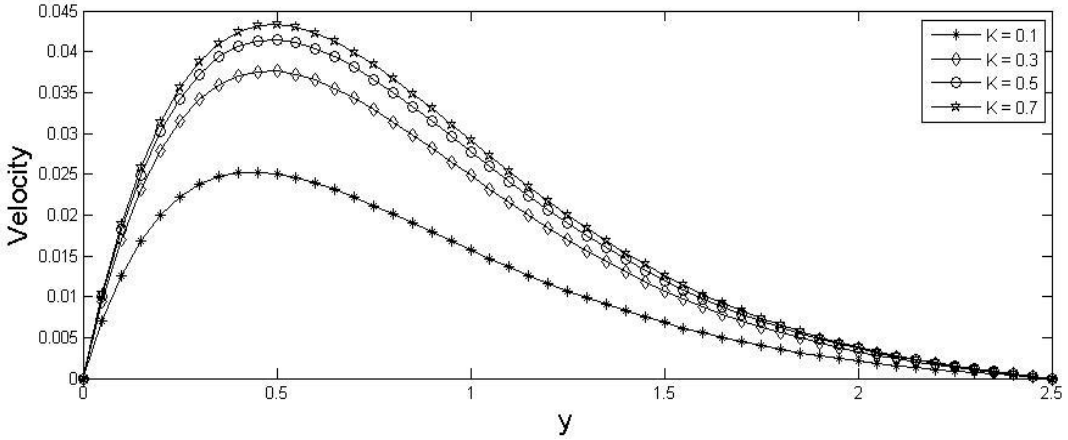

Figure 4: Variation of Velocity against y for different values of K.

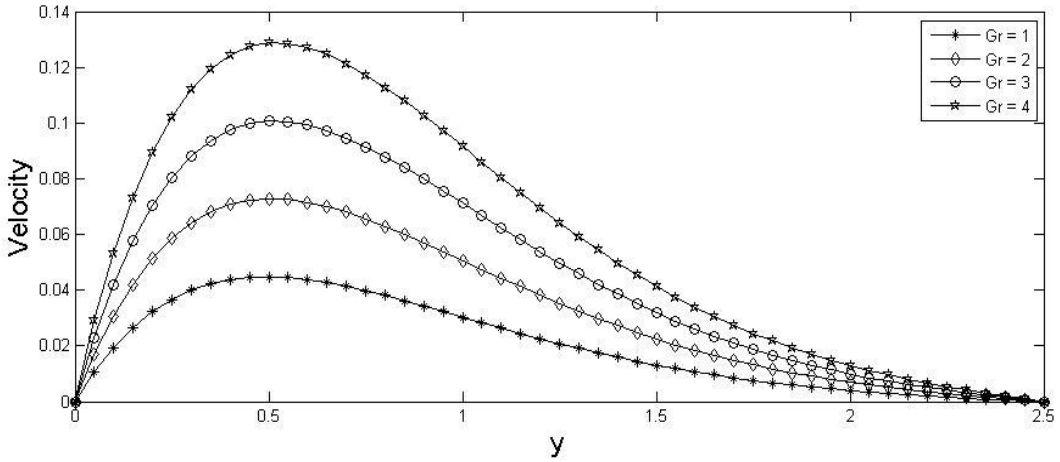

Figure 5: Variation of Velocity against y for different values of Gr.

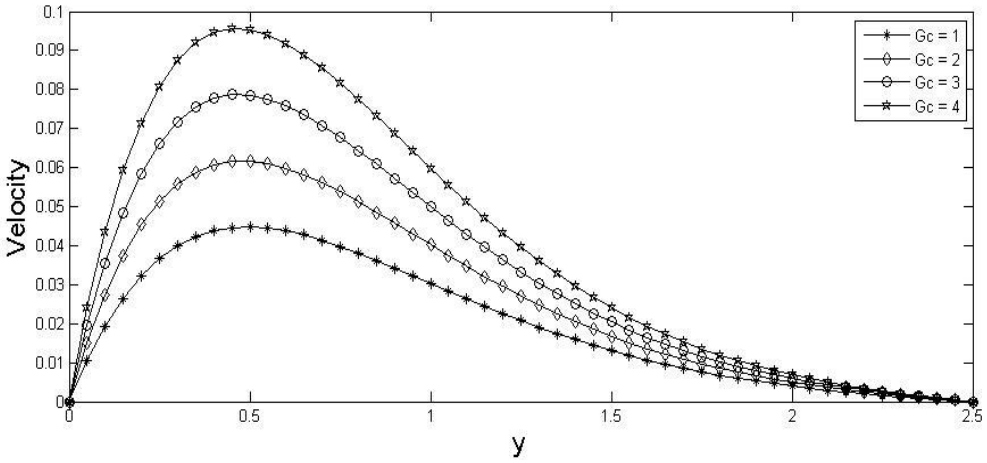

Figure 6: Variation of Velocity against y for different values of Gc.

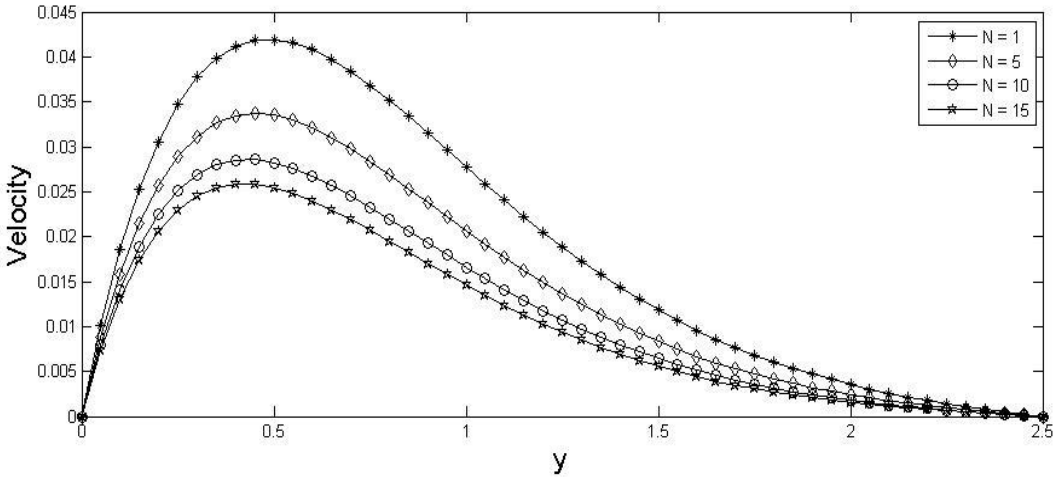

Figure 7: Variation of Velocity against y for different values of N.

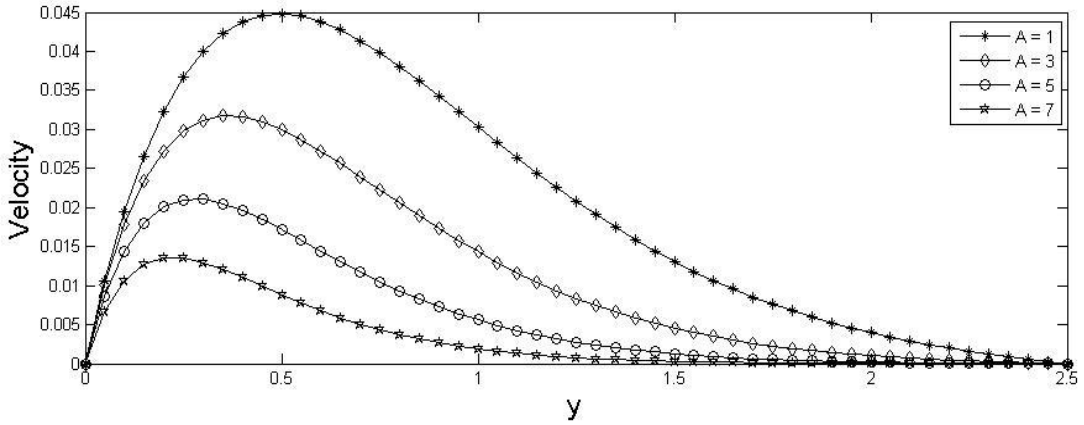

Figure 8: Variation of Velocity against y for different values of α .

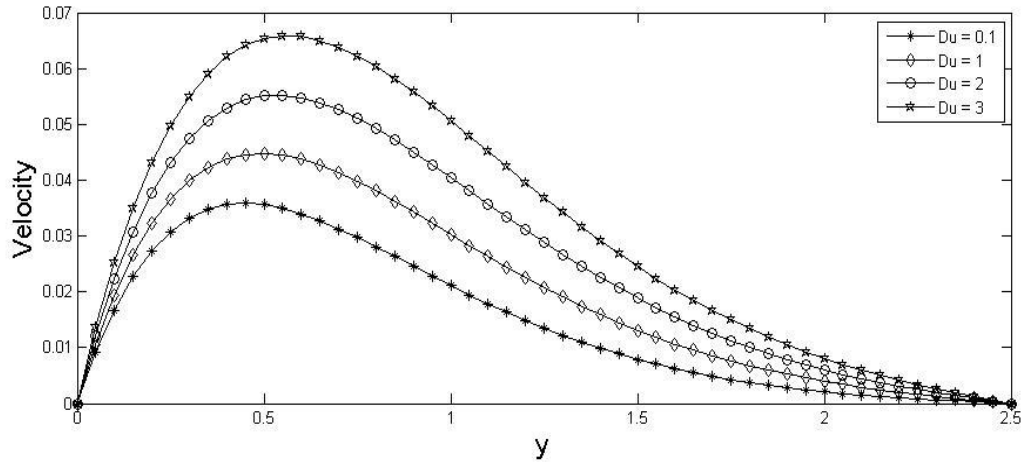

Figure 9: Variation of Velocity against y for different values of Du.

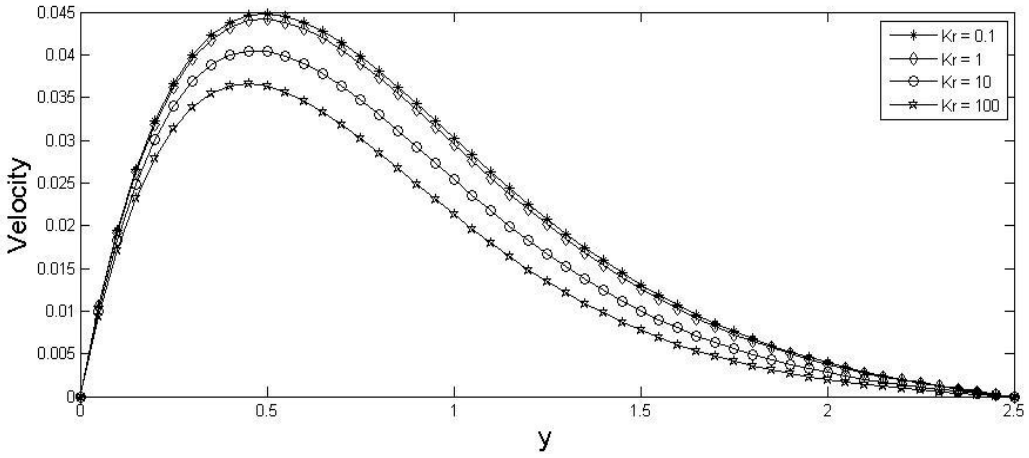

Figure 10: Variation of Velocity against y for different values of Kr.

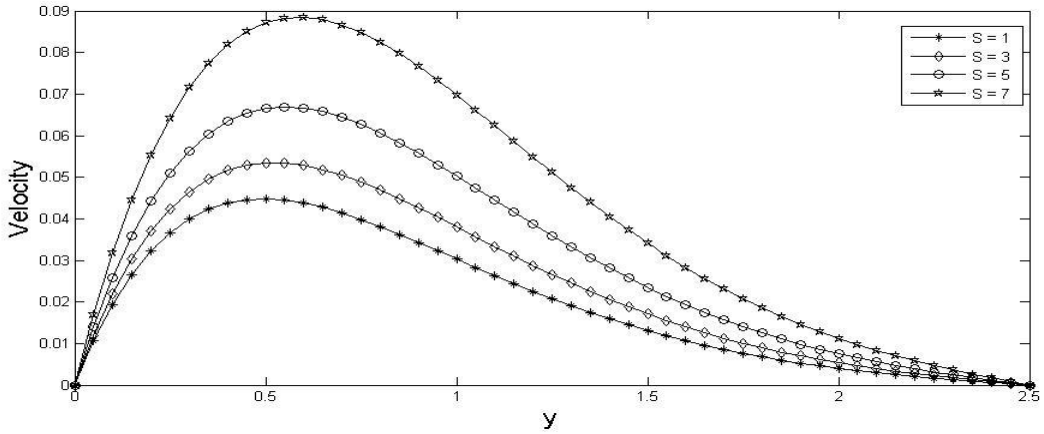

Figure 11: Variation of Velocity against y for different values of S.

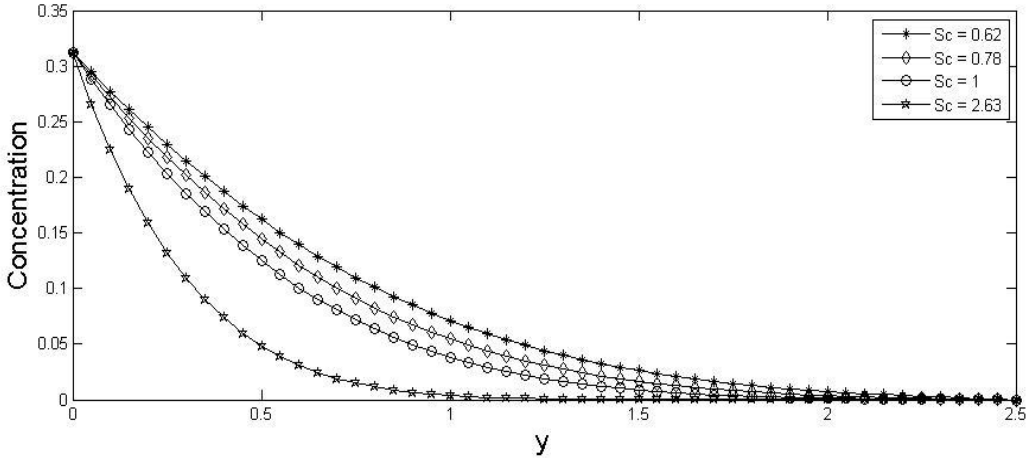

Figure 12: Variation of Concentration against y for different values of Sc.

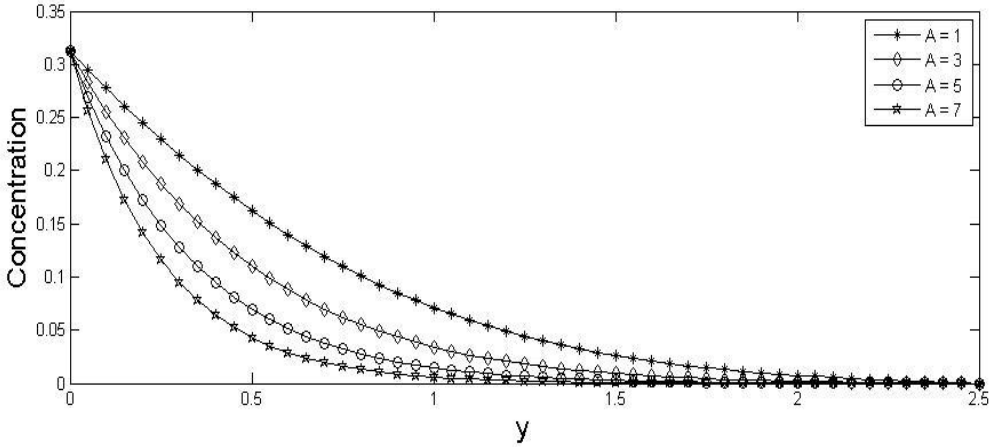

Figure 13: Variation of Concentration against y for different values of α .

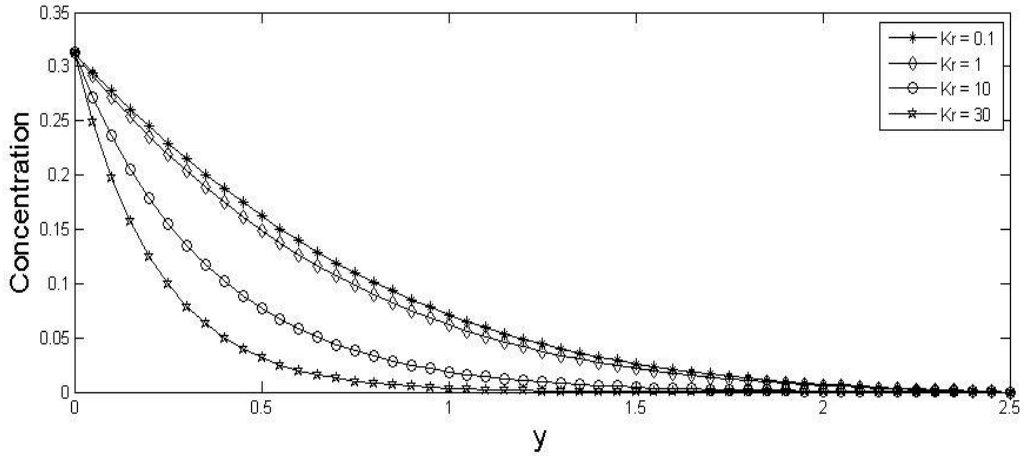

Figure 14: Variation of Concentration against y for different values of Kr.

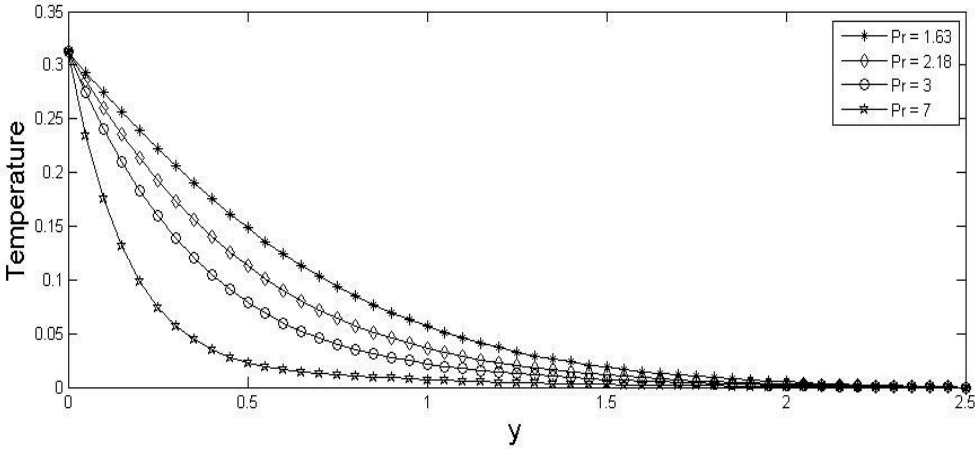

Figure 15: Variation of Temperature against y for different values of Pr.

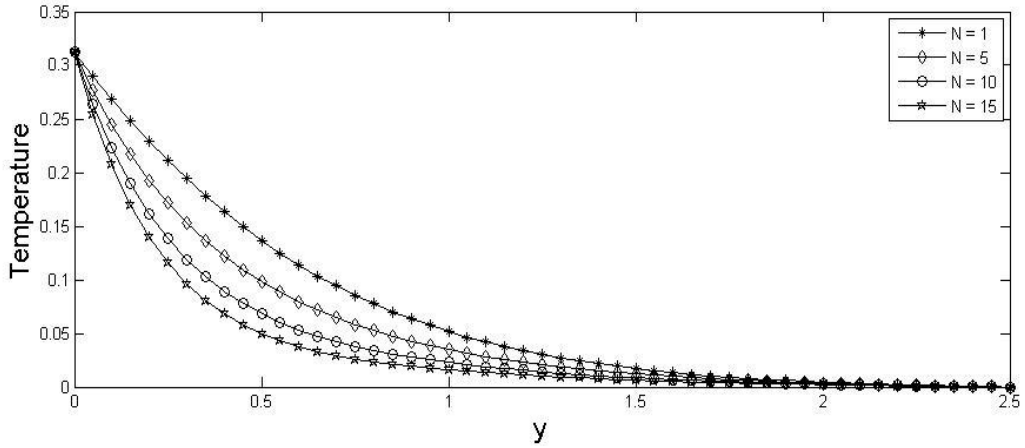

Figure 16: Variation of Temperature against y for different values of N.

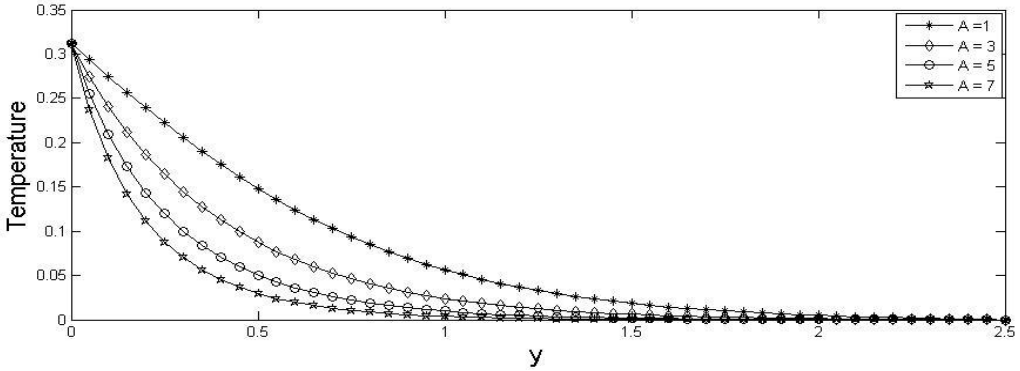

Figure 17: Variation of Temperature against y for different values of α .

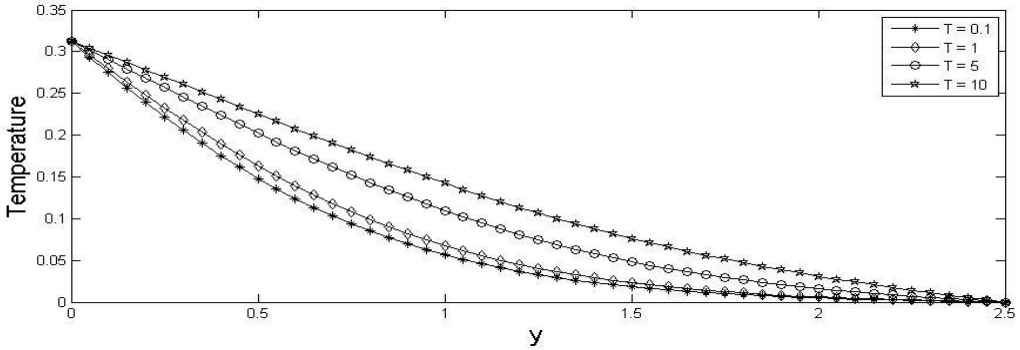

Figure 18: Variation of Temperature against y for different values of τ .

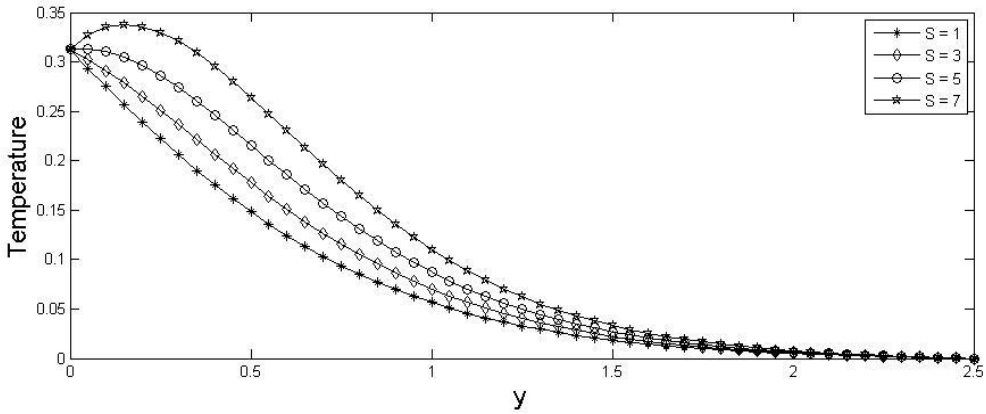

Figure 19: Variation of Temperature against y for different values of S.

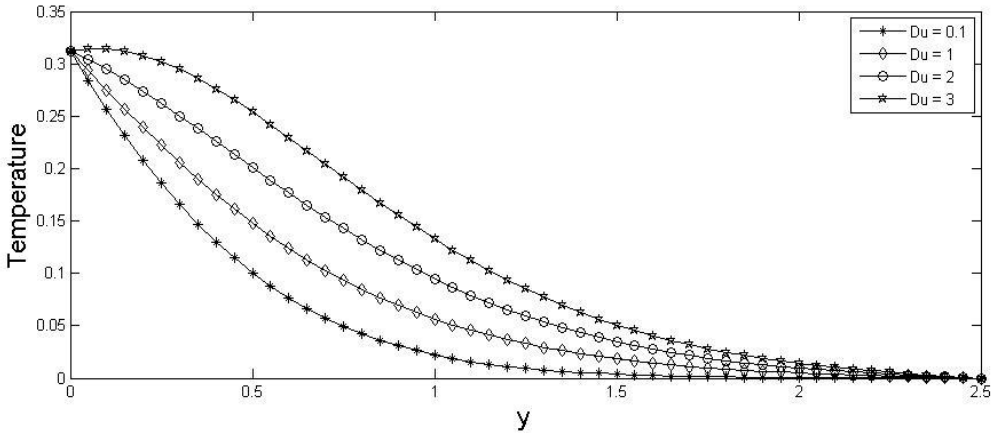

Figure 20: Variation of Temperature against y for different values of Du.

Table 1: Skin friction for different values of Pr, Gr, Gc, Sc, Kr, α , M, N and S.

Pr	Gr	Gc	Sc	Kr	α	M	N	S	C_f
0.71	1	1	0.62	0.1	1	1	0.1	1	0.2310
1	1	1	0.62	0.1	1	1	0.1	1	0.2134
0.71	5	1	0.62	0.1	1	1	0.1	1	0.7617
0.71	1	5	0.62	0.1	1	1	0.1	1	0.6243
0.71	1	1	0.78	0.1	1	1	0.1	1	0.2280
0.71	1	1	0.62	1	1	1	0.1	1	0.2292
0.71	1	1	0.62	0.1	4	1	0.1	1	0.2160
0.71	1	1	0.62	0.1	1	5	0.1	1	0.1902
0.71	1	1	0.62	0.1	1	1	1	1	0.2216
0.71	1	1	0.62	0.1	1	1	0.1	3	0.2585

Table 2: Nusselt number for different values of Pr, τ , N, n and α .

Pr	τ	N	n	α	-(Nu)
0.71	0.1	0.1	1	1	0.0050
1	0.1	0.1	1	1	0.1434
0.71	1	0.1	1	1	0.0143
0.71	0.1	1	1	1	0.1484
0.71	0.1	0.1	5	1	0.0109
0.71	0.1	0.1	1	4	0.0586

Table 3: Sherwood number for different values of Sc, Kr and α .

Sc	Kr	α	-(Sh)
0.62	0.1	1	0.3626
0.78	0.1	1	0.4218
0.62	1	1	0.4263
0.62	0.1	4	0.7663

VI. CONCLUSIONS

Dufour and heat source effects on heat mass transfer flow past an infinite vertical pate with variable thermal conductivity has been studied. Dimensionless governing equations were solved numerically using implicit finite difference scheme. Numerical solutions obtained are presented in graphs and tables for the fluid flow and heat mass transfer characteristics for different values of parameters involved in the problem. The present study will serve as a scientific tool for understanding more complex flow problems. The conclusion indicates that:

- The velocity increase whenever the thermal Grashof, mass Grashof and Dufour numbers, porosity and heat source parameters increases while it decrease with increasing Prandtl and Schmidt numbers, magnetic field, radiation, suction and chemical reaction parameters.
- The temperature increase for any increase in the thermal conductivity, Dufour number and heat source parameters but decrease with increasing Prandtl number, radiation and suction parameters.
- The concentration decrease with increase in Schmidt number, suction and chemical reaction parameters.
- The skin friction increase with increase of thermal Grashof number, mass Grashof number and heat source parameter but decreas when the Prandtl number, Schmidt number, chemical reaction, suction, magnetic field and radiation parameters increases. Whereas, the Nusselt number decrease whenever the Prandtl number, thermal conductivity, radiation, reaction order and suction parameters increased as in the Sherwood number which decrease with increase of any of the Schmidt number, chemical reaction and suction parameters.

REFERENCES

[1] Al-Odat, M. Q. and Al-Azab, T. A. (2007). Influence of chemical reaction on transient MHD free convection over a moving vertical plate. *Emirates Journal of Engineering Research*, **12(3)**: 15–21.

[2] Alam, M. S. and Rahman, M. M. (2006). Dufour and Soret effects on mixed convection flow past a vertical porous flat plate with variable suction. *Nonlinear Analysis: Modelling and Control*, **11(1)**: 3–12.

[3] Alam, M. S., Rahman, M. M., Ferdows, M. K., Koji, M. E. and Postelnicu, A. (2007).

[4] Diffusion-thermo and thermal-diffusion effects on free convective heat and mass transfer flow in a porous medium with time dependent temperature and concentration. *International Journal of Applied Engineering Research*, **2(1)**: 81–96.

[5] Anghel, M., Takhar, H. S. and Pop, I. (2000). Dufour and Soret effects on free convection boundary layer over a vertical surface embedded in a porous medium. *Studia Universitatis Babes-Bolyai, Mathematica* **XLV(4)**: 11–21.

[6] Bég, O. A., Bhargava, R., Rawat, S., Takhar, H. S. and Bég, T. A. (2007). A study of buoyancy-driven dissipative micropolar free convection heat and mass transfer in a Darcian porous medium with chemical reaction. *Nonlinear Analysis: Modeling and Control Journal*, **12(2)**: 157-180.

[7] Bég, O. A., Takhar, H. S., Kumari, M. and Nath, G. (2001). Computational fluid dynamics modeling of buoyancy-induced viscoelastic flow in a porous medium with magnetic field effects. *International Journal of Applied Mechanics and Engineering*, **6(1)**: 187-210.

[8] Choudhary, R. C. and Sharma, B. K. (2006). Combined heat and mass transfer by laminar mixed convection flow from a vertical surface with induced magnetic field. *Journal of Applied Physics*, **99**: 34901–10.

[9] Dursunkaya, Z. and Worek, W. M. (1992). Diffusion-thermo and thermal-diffusion effects in transient and steady natural convection from a vertical surface. *International Journal of Heat Mass Transfer*, **35**: 2060–2065.

[10] Hossain, M. M. T. and Khatun, M. (2010). Dufour Effect on Combined Heat and Mass Transfer by Laminar Mixed Convection Flow from a Vertical Moving Surface under the Influence of an Induced Magnetic Field. *Journal of Engineering Science*, **1(1)**: 23–38.

[11] Ibrahim, F. S., Elaiw, A. M. and Bakr, A. A. (2008). Effect of the chemical reaction and radiation absorption on the unsteady MHD free convection flow past a semi infinite vertical permeable moving plate with heat source and suction. *Communications in Nonlinear Science: Numerical Simulation*, **13(6)**: 1056–1066.

[12] Kafoussias, N. G. and Williams, E. W. (1995). Thermal-diffusion and diffusion-thermo effects on mixed free-forced convective and mass transfer boundary layer flow with temperature dependent viscosity. *International Journal of Engineering Science*, **33**: 1369–1384.

[13] Muthucumarswamy, R. (2009). First order chemical reaction on exponentially accelerated isothermal vertical plate with mass diffusion. *Annals Faculty of Engineering, Hunedoara, Tome,* **(7)**: 47-50.

[14] Moller, M. M., Rahman, A. and Rahman L. T. (2005). Natural convection flow from an isothermal sphere with temperature dependent thermal conductivity. *Journal of Naval Architecture and Marine Engineering*, **2(2)**: 53-64.

[15] Pantokratoras, A. (2007). Comment on "Combined heat and mass transfer by laminar mixed convection flow from a vertical surface with induced magnetic field". *Journal of Applied Physics*, **102**: 076113.

[16] Postelnicu, A. (2004). Influence of a magnetic field on heat and mass transfer by natural convection from vertical surfaces in porous media considering Soret and Dufour effects. *International Journal of Heat and Mass Transfer*, **47**: 1467–1472.

[17] Rajesh, V. and Varma, S. V. K. (2009). Chemical reaction and radiation effects on MHD flow past an infinite vertical plate with variable temperature. *Far East Journal of Mathematical Sciences*, **32(1)**: 87-106.

[18] Rawat, S. and Bhargava, R. (2009). Finite element study of natural convection heat and mass transfer in a micropolar fluid-saturated porous regime with Soret/Dufour effects. *International Journal of Applied Mathematics and Mechanics*, **5(2)**: 58–71.

[19] Souza, M., De Ulson, A. G. and Whitaker, S. (2003). Mass transfer in porous media with heterogeneous chemical reaction. *Brazilian Journal of Chemical Engineering*, **20(2)**: 191-199.

[20] Stangle, G. C. and Aksay, I. A. (1990). Simultaneous momentum, heat and mass transfer with chemical reaction in a disordered porous medium: application to binder removal from a ceramic green body. *Chemical Engineering Science*, **45(7)**: 1719-1731.

[21] Trevisan, O. V. and Bejan, A. (1990). Combined heat and mass transfer by natural convection in a porous medium. *Advance Heat Transfer*, **20**: 315-352.